Current and Thermal Quench in JET and ITER Disruptions

H. Strauss[1], S. Jardin[2], JET contributors[3]

[1] *HRS Fusion, West Orange USA*

[2] *PPPL, Princeton, USA*

[3] *See the author list of 'Overview of JET results for optimizing ITER operation' by J Mailloux et al., to be published in Nucl Fusion Special Issue: Overview and summary papers from the 28th FEC 2021*

Self mitigation of asymmetric wall force in asymmetric vertical displacements (AVDE) and of thermal quench in locked mode disruptions is presented. Theory and simulations are compared to JET experimental results, and applied to ITER.

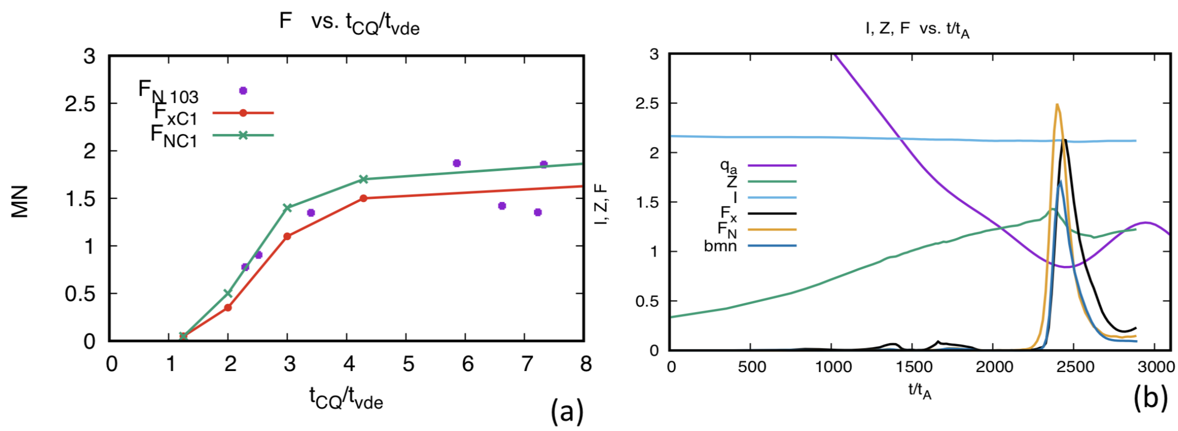

Figure 1: (a) shows sideways force F_{xC1} calculated with M3D-C1, the Noll force FN_{103}, from JET ILW disruption database 2011-16, and F_{Nc1} calculated with M3D-C1. The sideways force is eliminated if CQ time < VDE time. (b) shows current I, vertical position Z, q_a, the sideways and Noll forces, and the energy of magnetic modes b_{mn}.

There are two main possible kinds of damage from ITER disruptions. Electromechanical damage can be caused by asymmetric wall force in asymmetric vertical displacements (AVDE). It has been shown that if the current quench (CQ) time is sufficiently short, the asymmetric wall force does not occur [7, 9]. Recently the detailed mechanism of the asymmetric wall force has been presented [1].

A thermal quench (TQ) can cause excessive heat load and melting of the divertor wall material. Recently it was shown that the TQ in JET locked mode disruptions is caused by a resistive wall tearing mode (RWTM) [3]. In ITER the RWTM is slowly growing, and it is possible that ITER might not experience a rapid TQ as in present experiments. In ITER, there might be only disturbances, rather than disruptions.

Fig.(a) shows sideways force F_{xC1} calculated with M3D-C1 [2], the Noll force FN_{103} from JET ILW disruption database 2011-16, and F_{Nc1} calculated with M3D-C1. The Noll force is $F_N = \pi B \Delta M_{IZ}$, with $M_{IZ} = IZ$, the product of toroidal current and vertical displacement, and Δ is the r.m.s toroidal variation. The sideways force is eliminated if the CQ time < VDE time. Fig.(b) shows the mechanism of sideways force. In the case the current I is held constant, and not quenched. The vertical displacement Z increases in time and then saturates. Magnetic flux is scraped off at the wall, and the plasma cross section shrinks, causing the value q_a at the wall to drop. When $q_a = 1$, this excites a (1,1) external kink. The asymmetric and Noll forces, and the energy of magnetic modes b_{mn} increase together, then saturate and decay. If there is a CQ, there is less current by the time the VDE saturates. In ITER, the CQ time would be expected to be less than the VDE time, and the asymmetric wall force will be small.

The second topic is the TQ. Fig.(a) shows a locked mode in JET shot 81540. The locked mode magnetic signal B_{ML} is small, then increases. This is the disruption precursor. Then there is a rapid spike, which is the TQ. Also shown in T_{20}, the temperature near the plasma center at radius $r \approx 0.2a$. Fig.(b) is a closeup in time of the TQ, measured in units of resistive wall penetration time $\tau_{wall} = 5ms$. The TQ is caused by the growth and saturation a magnetic instability, with growth time $\gamma^{-1} = 0.3\tau_{wall} = 1.5ms$, which is also the TQ time, $\tau_{TQ} = \gamma^{-1}$.

Theory and simulations show that this is a RWTM, with growth rate

$$\gamma\tau_A = c_0 S^{-1/3} S_{wall}^{-4/9} \tag{1}$$

where in this case $c_0 \approx 2$, and $\tau_A = R/v_A$ is the Alfvén time, S is the Lindquist number, and $S_{wall} = \tau_{wall}/\tau_A$. Fig.(a) shows the time history of total P and wall magnetic perturbations b_n

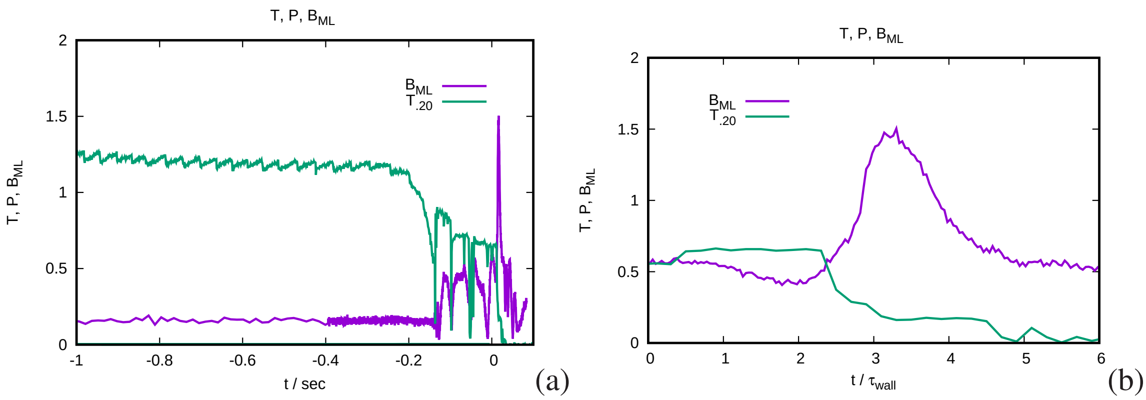

Figure 2: (a) history of a JET locked mode disruption showing precursor and TQ (b) TQ resolved with time in units of wall time $\tau_{wall} = 5ms$.

for an M3D [6] simulations with $S_{wall} = 10^3, 10^4, 10^5$ and $S = 10^6$. For larger S_{wall}, P decays more slowly, and b_n increases more slowly. Here b_n is the r.m.s. perturbed 3D normal magnetic field at the wall, normalized to the toroidal magnetic field. Fig.(b) collects TQ time τ_{TQ} in Alfvén time units as a function of S_{wall}. The curve is fitted to a RWTM growth time. For large S_{wall} the RWTM not important and τ_{TQ} is independent of S_{wall}. The left vertical line is JET value, and the right is ITER. Linear simulations verify $S^{-1/3}$ scaling of RWTM growth rate. The TQ time τ_{TQ} is given by the smaller of $1/\gamma$ or the parallel thermal transport time

$$\tau_{TQ} \approx \left(\frac{1}{\gamma}, \tau_{\|}\right)_{min} \quad (2)$$

where $\tau_{\|} = a^2/(\chi_{\|} b_{n0}^2)$, $\chi_{\|}$ is the parallel thermal diffusivity in the plasma edge region, b_n is the root mean square amplitude of magnetic perturbations normal to the plasma boundary, b_{n0} is the precursor amplitude of b_n when the RWTM is negligible, and a is the minor radius in the midplane.

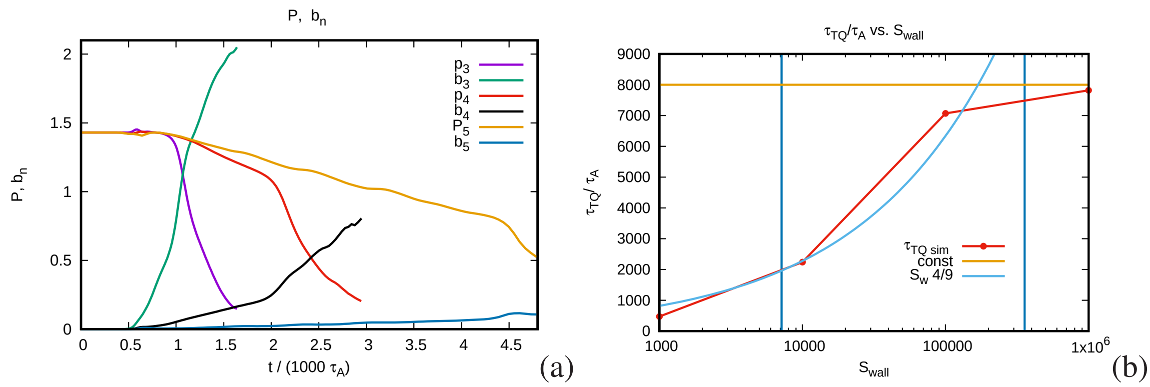

Figure 3: (a) time history of total P and wall magnetic perturbations b_n for simulations with $S_{wall} = 10^3, 10^4, 10^5$. (b) τ_{TQ} in Alfvén time units as a function of S_{wall}.

The formula (2) may be applied to examine the effect of using realistic parameters, in particular the dependence of τ_{TQ} on T and b_n. $\chi_{\|} = (2/3)\kappa_{\|}/n = 2.1 v_e^2 \tau_e$, A combined form of $\chi_{\|}$ with both collisionless and collisional limits is

$$\chi_{\|} = \frac{\pi R v_e}{1 + \pi R/(2.1 v_e \tau_e)} \quad (3)$$

Fig. shows TQ in ITER for $0.001 \le T/100eV \le 10$. The curve $1/\gamma_1$ has ITER values $S_{wall} = 3.5 \times 10^5$, $c_0 = .51$, and $1/\gamma_2$ has the JET value [3] $S_{wall} = 7 \times 10^3$, $c_0 = 2.2$. The $\tau_{\|}$ curves are $\tau_{\|1}$ with $b_n = 10^{-3}$, and $\tau_{\|2}$ with $b_n = 2 \times 10^{-3}$. The TQ time given by (2). The value $\tau_{TQ} = 10ms$ is also shown. It is clear from Fig.4 that there are two different temperature regimes. In the collisionless regime the condition $\tau_{\|} \ge 10ms$ requires that $T/T_0 \le 26(b_0/b_n)^4$. In this regime

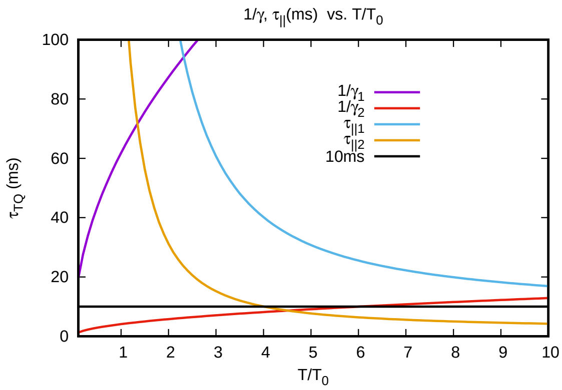

Figure 4: $\tau_{||}$ *and* $1/\gamma$, *where* $1/\gamma_1$ *is for ITER with* $S_{wall} = 3.5 \times 10^5$, $c_0 = .51$, *and* $1/\gamma_2$ *is for JET, with* $S_{wall} = 7 \times 10^3$, $c_0 = 2.2$. *The* $\tau_{||}$ *values are* $\tau_{||1}$ *with* $b_n = 10^{-3}$, *and* $\tau_{||2}$ *with* $b_n = 2 \times 10^{-3}$.

τ_{TQ} is very sensitive to b_n. In the collisional regime, $T < 325eV$, the criterion is approximately $T/T_0 \leq 4.9(b_0/b_n)^{4/5}$, a much weaker scaling with b_n. The simulations presented here give $b_n = b_0 = 10^{-3}$. This agrees with an empirical scaling of locked mode perturbation amplitudes B_{ML} before the TQ [4]. Another estimate [4] assumes a maximum island width $w/a = 0.3$, giving $b_n = 2 \times 10^{-3}$.

Acknowledgment Work supported by USDOE grant DE-SC0020127, Contracts No. DE-AC02-09CH11466, and No. DE-SC0018001. This work has been carried out within the framework of the EUROfusion Consortium and has received funding from the Euratom research and training programme 2014-2018 and 2019-2020 under grand agreement No 633053. The views and opinions expressed herein do not necessarily reflect those of the European Commission

References

[1] S. C. Jardin *et al.*, IAEA 28th Fusion Energy Conference, 12 May 2021, P3 posters 3, 853.

[2] S. C. Jardin, N. Ferraro, J. Breslau *et al.*, Comput. Sci. & Disc., 5 p 014002 (2012)

[3] H. Strauss and JET Contributors, Phys. Plasmas **28**, 032501 (2021)

[4] P.C. de Vries *et al.*, Nucl. Fusion **56** 026007 (2016)

[5] T.C. Hender *et al.*, Nucl. Fusion 47 S128 (2007)

[6] W. Park, *et al.*Phys. Plasmas **6** 1796 (1999).

[7] H. Strauss,

[8] H. Strauss, E. Joffrin, V. Riccardo, J. Breslau, R. Paccagnella, G.Y. Fu, and JET contributors, Phys. Plasmas **27** 022508 (2020)

[9] H. Strauss, E. Joffrin, V. Riccardo, J. Breslau, R. Paccagnella, and JET Contributors, Phys. Plasmas **24** 102512 (2017).